

A transportable optical lattice clock

Stefan Vogt, Jacopo Grotti, Silvio Koller, Sebastian Häfner, Soia Herbers, Sören Dörscher, Uwe Sterr and Christian Lisdat

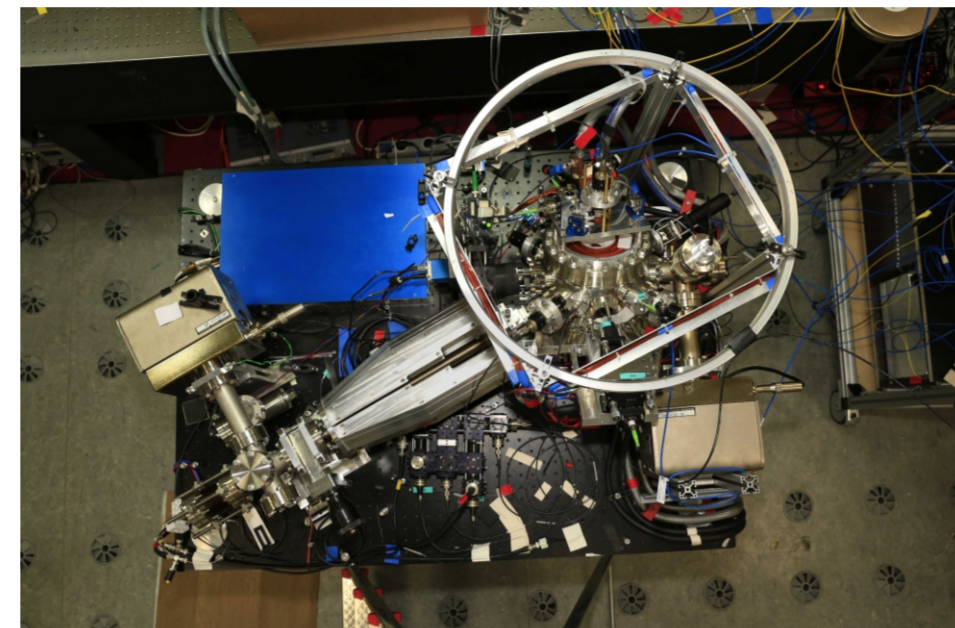
Transportable clocks

Clocks that can be operated outside the laboratory are needed for:

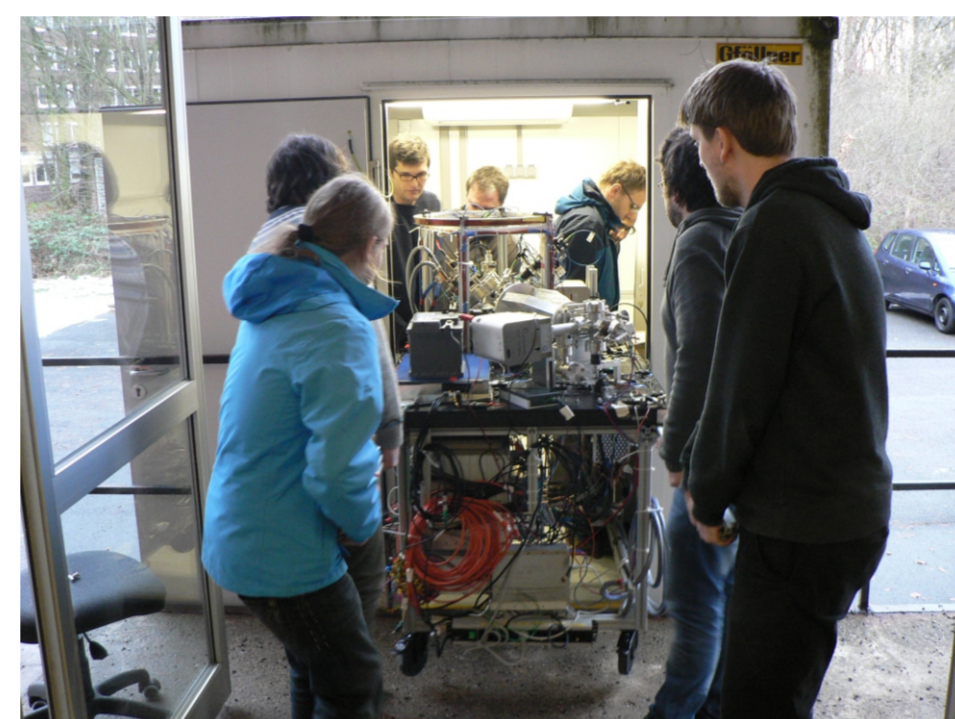
- ▶ Direct comparisons of optical frequencies without reference to Cs primary clocks.
- ▶ Frequency comparisons between distant experiments.
- ▶ Local measurements of the geo-potential (chronometric levelling, relativistic geodesy).

Proof-of-principle experiment (February–March 2016):

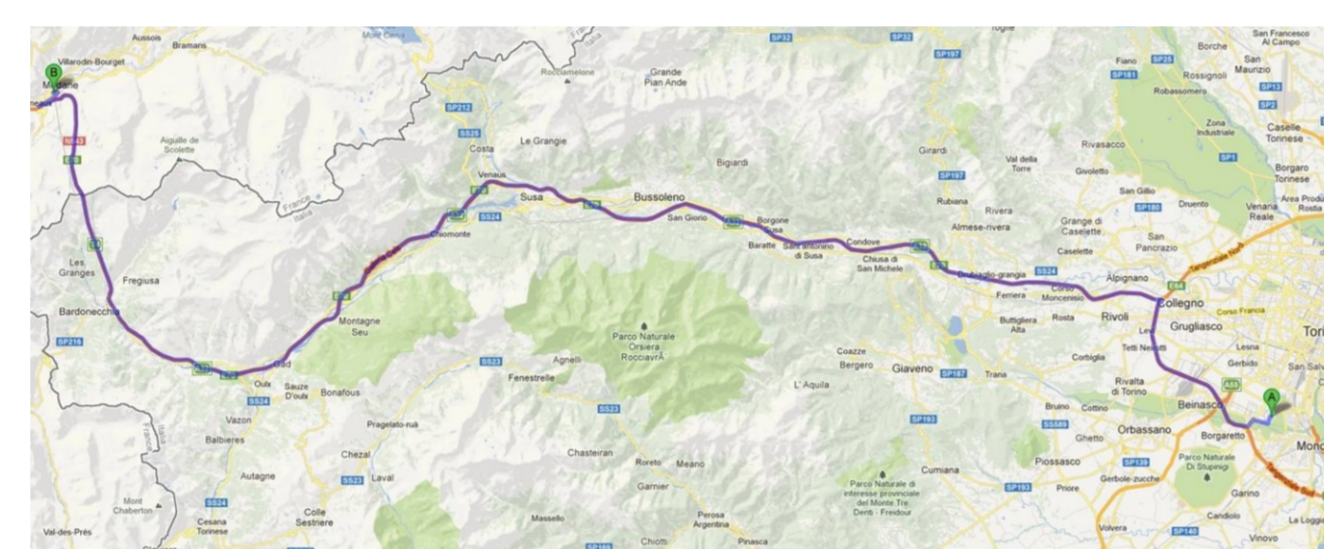
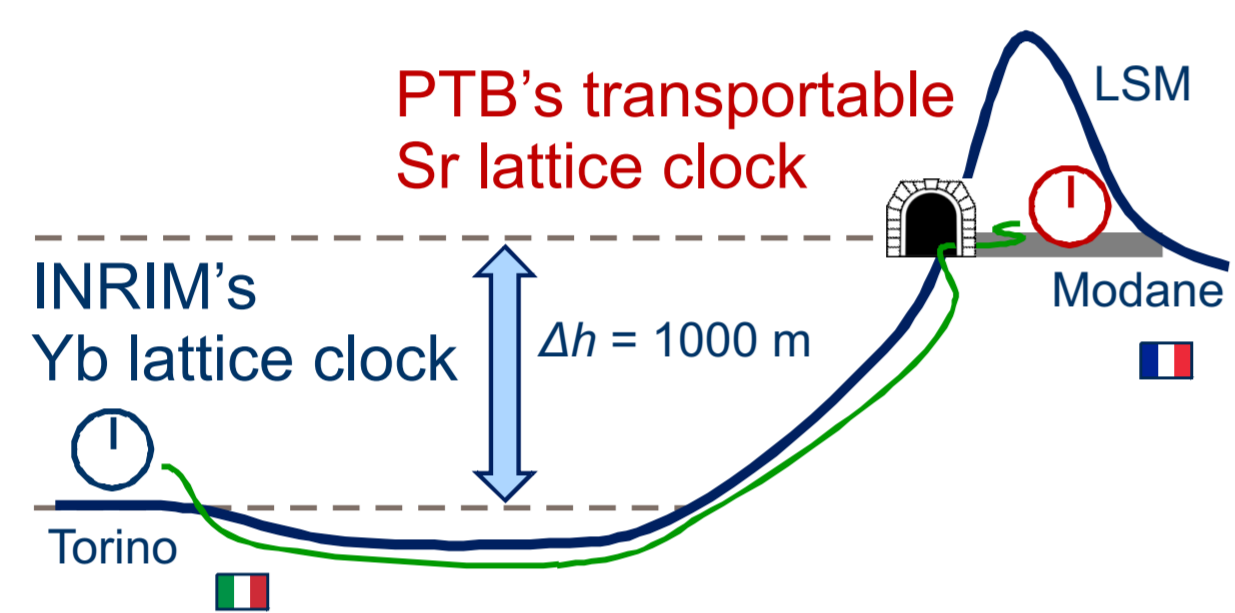
- ▶ Measure 1000 m height difference with 0.5 m uncertainty, (i.e., $5 \cdot 10^{-17}$ fractional frequency uncertainty in red shift) by comparison of two optical clocks over a 100 km fibre link.
- ▶ Part of the EMRP project *International Timescales with Optical Clocks (ITOC)*.
- ▶ Close collaboration with geodesists at Leibniz Universität Hannover within *CRC 1729 geo-Q*.



Physics package of the transportable clock.



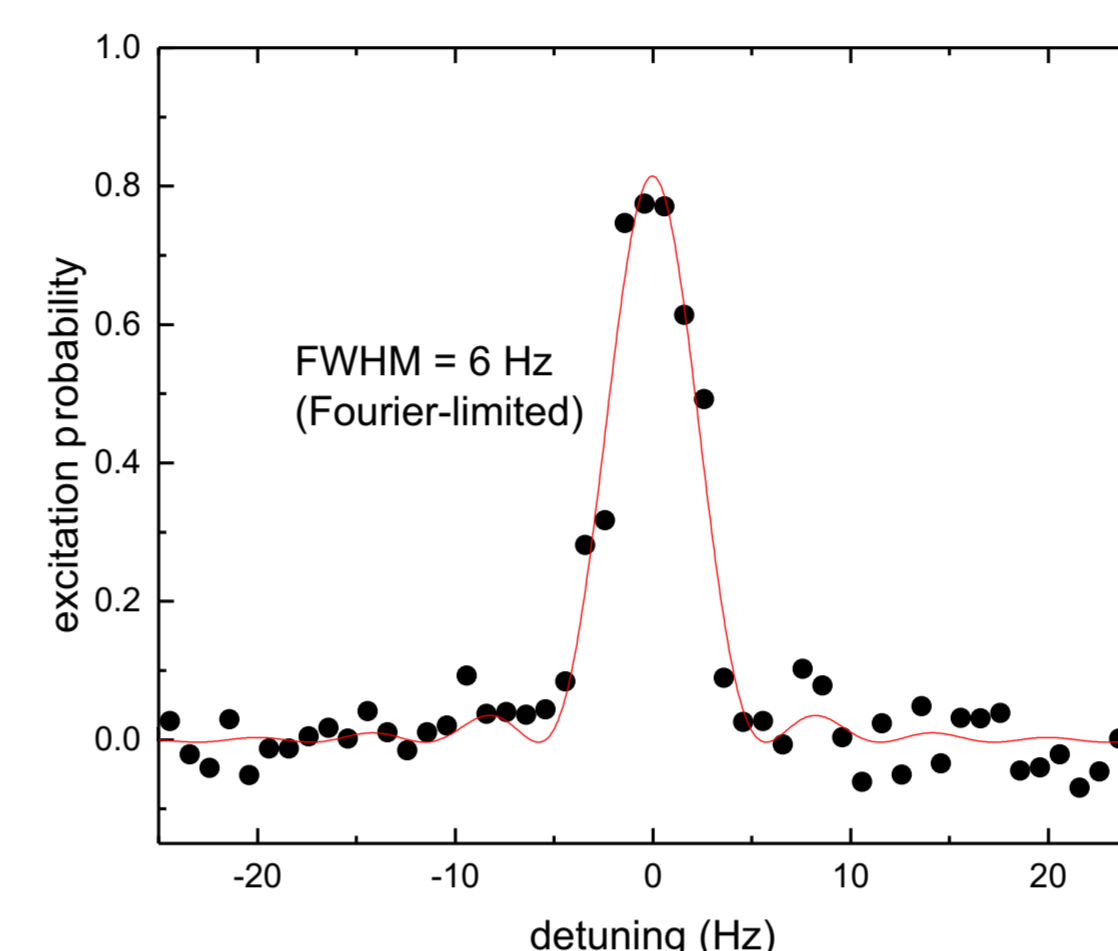
The clock being moved to the trailer for transport.



Spectroscopy of ^{87}Sr in a lattice at 813 nm

Clock transition with transportable laser:

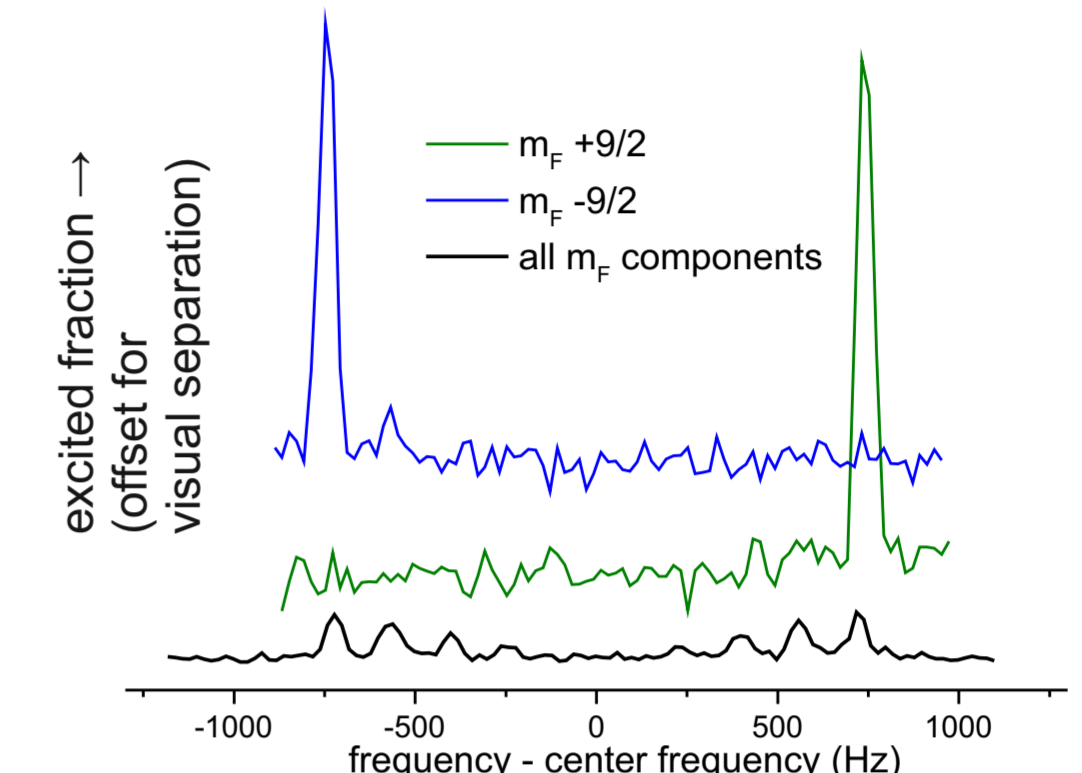
- ▶ A narrow line with a Fourier-limited width of 6 Hz (FWHM) has been obtained.



Scan of the clock transition.

Spin polarisation:

- ▶ Prepare atoms in $m_F = \pm 9/2$ for high contrast during spectroscopy.
- ▶ Optical pumping by σ -polarised light on the $^1S_0(F=9/2) \rightarrow ^3P_1(F'=9/2)$ transition at 689 nm.



Magnetic line splitting and effect of spin polarisation.

Recent progress

Laser cooling & trapping:

- ▶ Laser-cooled atoms loaded into optical lattice near magic wavelength ($\lambda_m \approx 813$ nm).
- ▶ High-resolution spectroscopy of the clock transition $^1S_0 \rightarrow ^3P_0$ in ^{87}Sr .
- ▶ Lamb-Dicke regime with resolved sidebands.
- ▶ Observed sideband frequencies match lattice parameters.

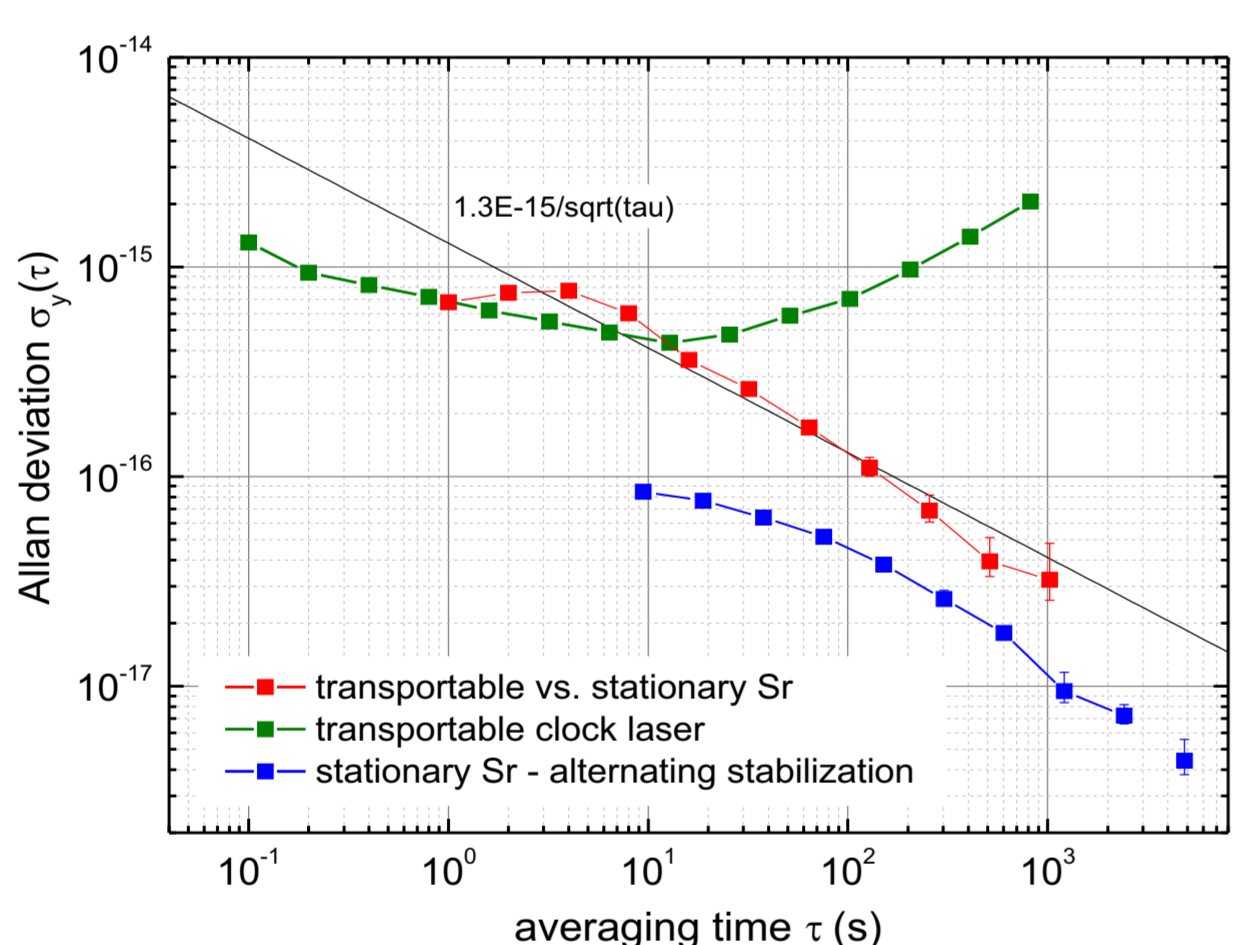
Clock operation:

- ▶ Clock laser stabilised to atomic transition.
- ▶ Preliminary evaluation of uncertainty budget.
- ▶ Side-by-side comparison with stationary clock performed.
- ▶ System in the field for first, proof-of-principle measurement campaign.

Accuracy and stability

Design goal for transportable clock:

Systematic uncertainty and instability comparable to state-of-the-art optical clocks.



Allan deviation of the ^{87}Sr lattice clocks' frequency ratio during comparison.

Preliminary uncertainty budget:

Effect	Correction (10^{-17})	Uncertainty (10^{-17})
BBR Stark shift (ambient)	488	1
BBR Stark shift (oven)	0	0.1
2 nd order Zeeman shift	11.1	0.5
Density shift	-1.2	3.1
Lattice shift, scalar/tensor	-8.9	6.4
Lattice shift, hyperpolarisability	-0.2	0.1
Total	488.8	7.1

Comparison with PTB's stationary clock:

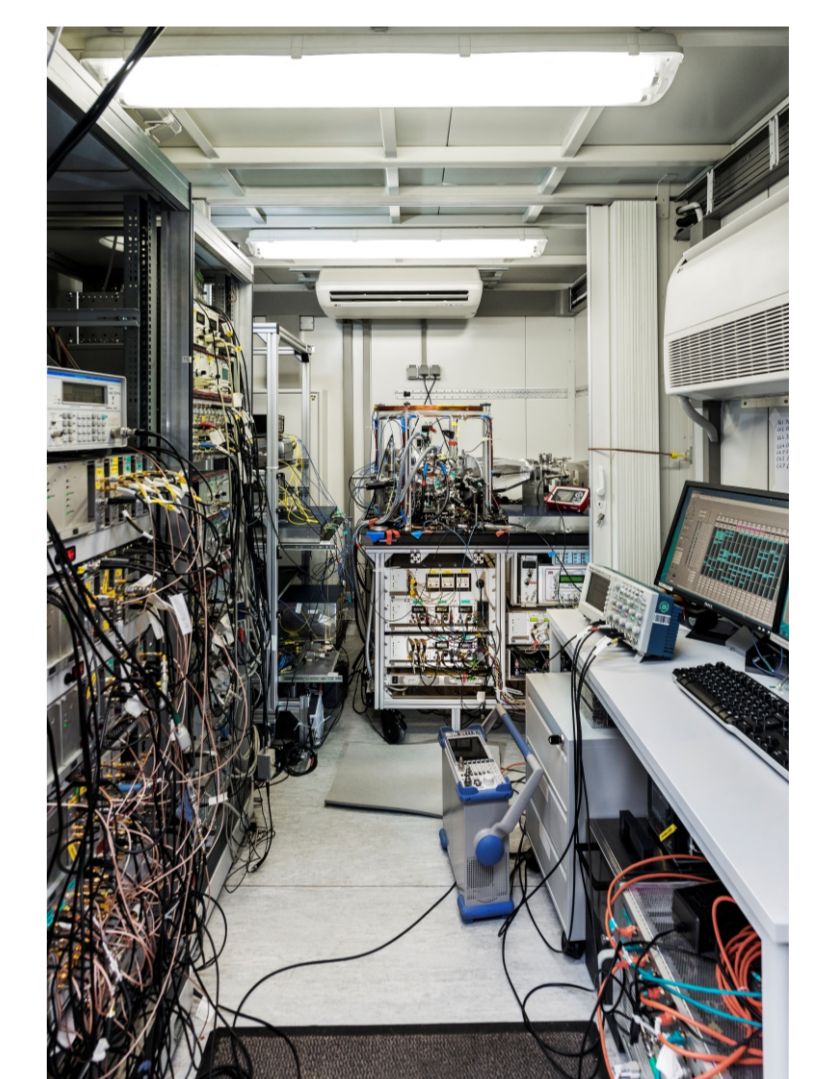
- ▶ **Stability limited by clock laser** (with frequency instability of $6 \cdot 10^{-16}$ at 1 s).
- ▶ **Clock instability of $1.3 \cdot 10^{-15} (\tau/s)^{-1/2}$** , reaching an uncertainty of $3 \cdot 10^{-17}$ after 1000 s of averaging.
- ▶ **Agreement with stationary clock:**
 $\nu(\text{Sr}_{\text{transportable}}) - \nu(\text{Sr}_{\text{stationary}}) = 2(3)_{\text{stat}} \cdot 10^{-17} \nu_0$

First measurement campaign

The clock has been moved into a trailer and transported to the *Laboratoire Souterrain de Modane (LSM)* for its first measurement campaign, together with NPL's transportable comb.



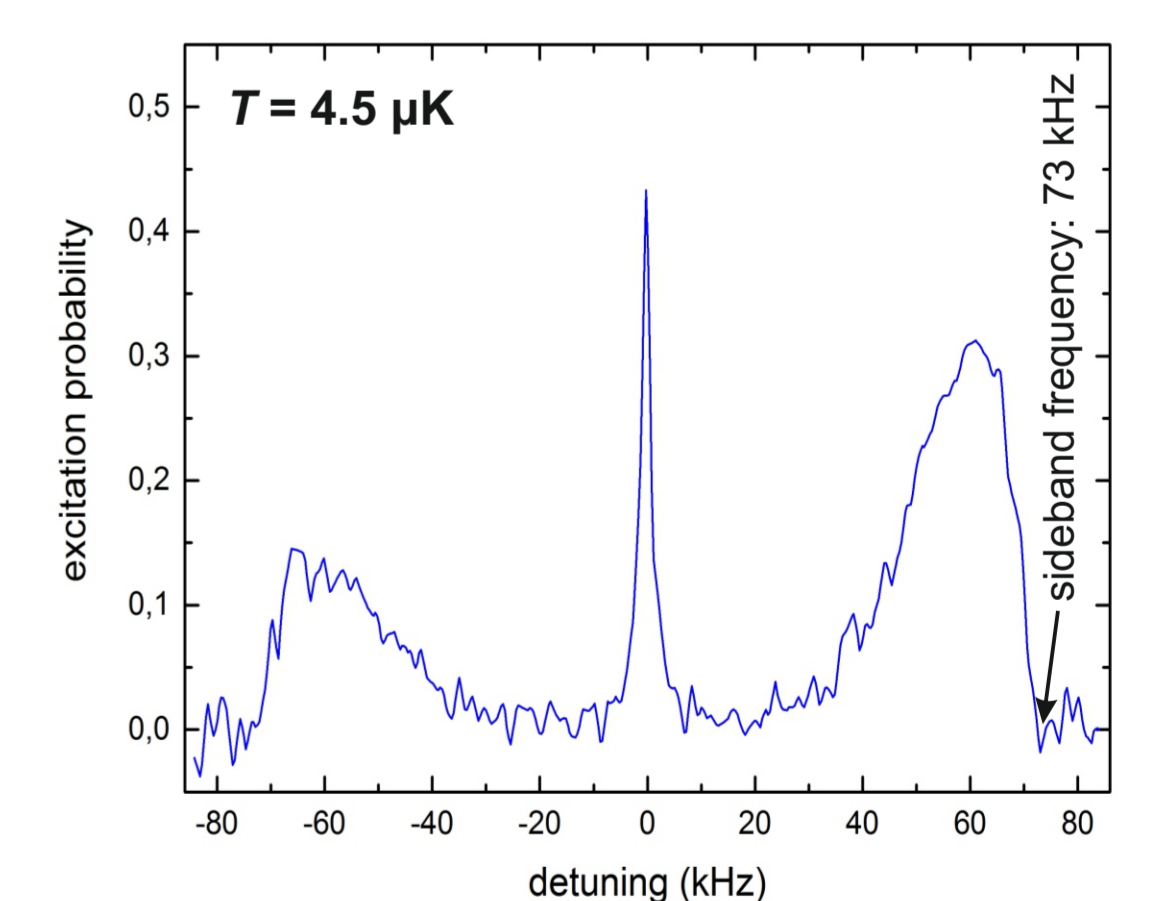
PTB's transportable clock (back) and NPL's transportable comb (front) settled in at LSM inside the Fréjus tunnel.



Interior of the trailer housing the experiment.

First results after transport to Modane:

- ▶ **One week after arrival:** ^{87}Sr atoms cooled and loaded into the lattice.
- ▶ **Ten days after arrival:** Clock transition found and sideband spectroscopy performed.
- ▶ **Measurement campaign still in progress!**



Sideband spectrum recorded at LSM.

Blackbody radiation-induced shift

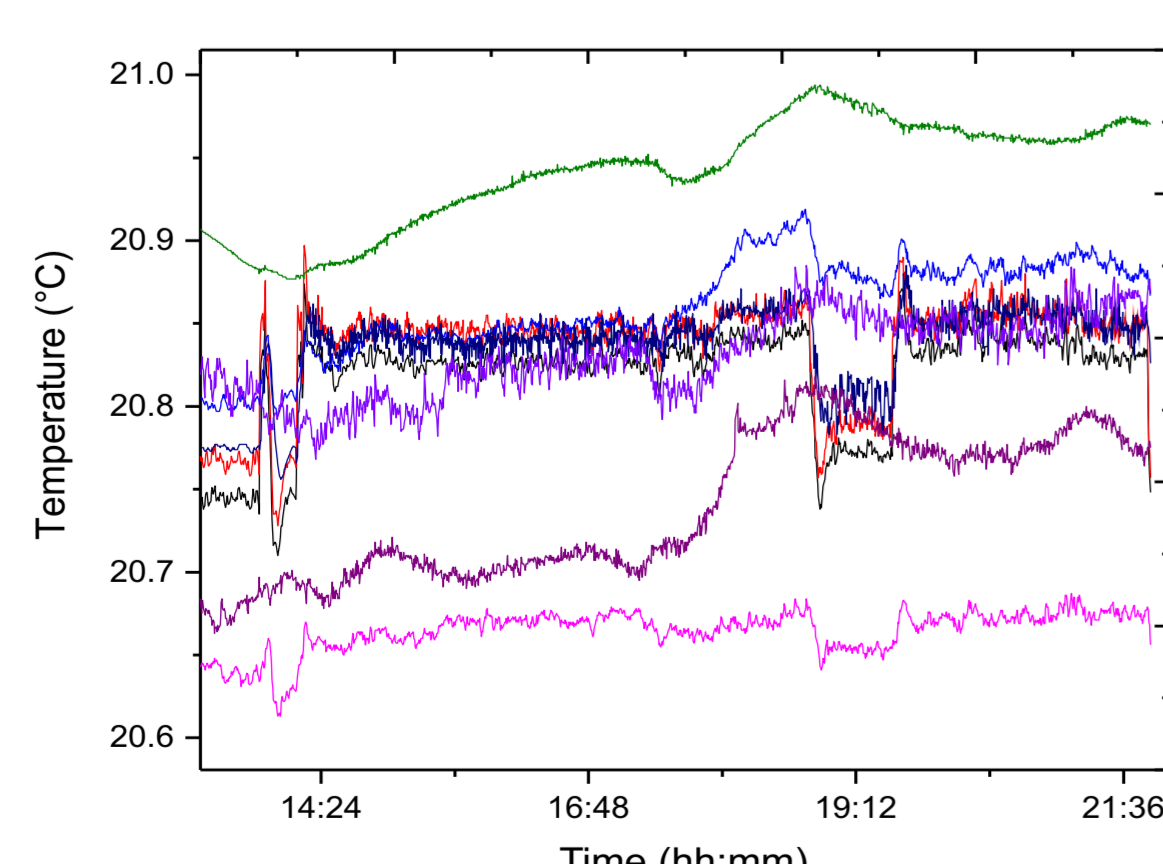
Quadrupole coil design:

- ▶ Power dissipation of ca. 80 W per coil in continuous operation (at 60 A current, generating a magnetic field gradient of ~ 7 mT/cm).
- ▶ Copper tubing with square cross section and large inner width allows efficient water cooling.
- ▶ Platinum-wire temperature sensors (Pt100) with 40 mK measurement uncertainty placed at critical locations.

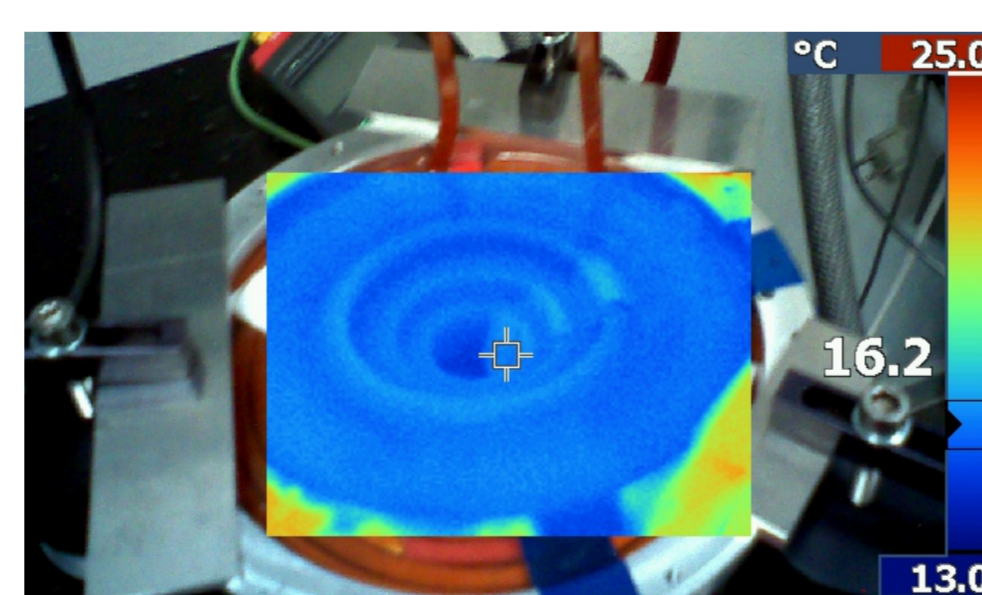
BBR-induced Stark shift:

$$\Delta\nu_{\text{BBR}}(T) = \alpha_{\text{stat}} (T/T_0)^4 + \alpha_{\text{dyn}} [(T/T_0)^5 + O((T/T_0)^6)]$$

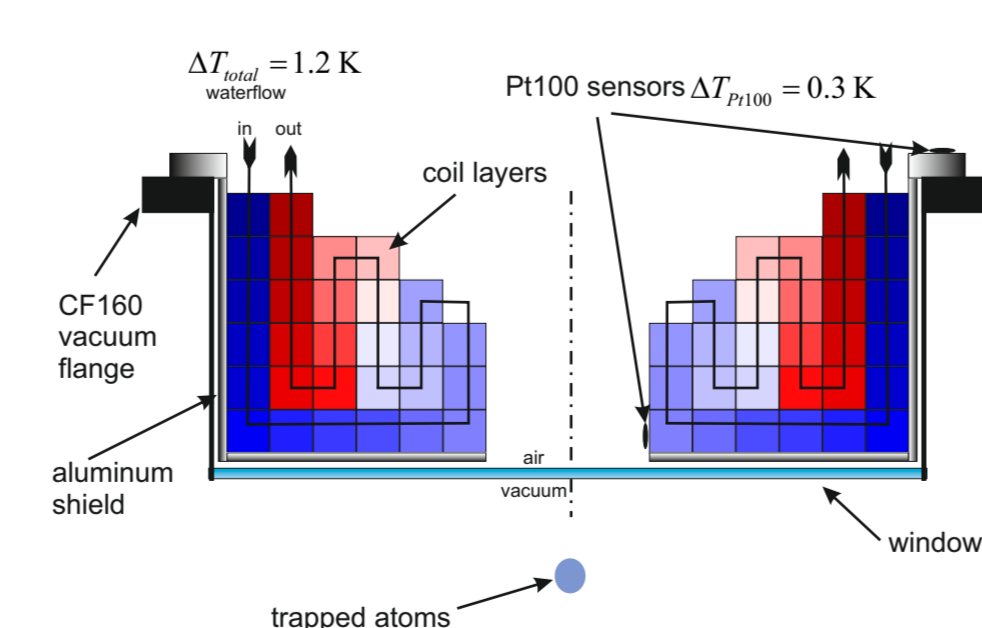
- ▶ Temperature gradient: $\Delta T_{\text{p-p}} = 480$ mK (including sensor uncertainty)
- ▶ **BBR shift uncertainty:** $u_B(\text{BBR}) = 1 \cdot 10^{-17}$



Thermal gradients during operation.



Thermal image of a coil.



Schematic view of a coil.

Future improvements

Reduced systematic uncertainty:

- ▶ Full evaluation of the magic wavelength.
- ▶ Improved analysis of density shifts.

Lower clock instability:

- ▶ New clock laser system based on a smaller and more stable cavity.

Better transportability and reliability:

- ▶ Optimisation of environmental conditions inside the trailer, e.g., by removing heat sources.
- ▶ Further size & weight reduction of the clock and lattice laser modules.
- ▶ Transition to a single red cooling laser with modulation sidebands (for cooling & stirring).